Article

A GABAergic Feedback Shapes Dopaminergic Input on the *Drosophila* Mushroom Body to Promote Appetitive Long-Term Memory

Highlights

- A feedback circuit between dopaminergic and GABAergic neurons consolidates memory

- Two antagonist dopamine receptors regulate the GABAergic neuron activity

- The GABAergic neuron regulates the calcium oscillations of the dopaminergic neuron

Authors

Alice Pavlowsky, Johann Schor, Pierre-Yves Plaçais, Thomas Preat

Correspondence

thomas.preat@espci.fr

In Brief

Pavlowsky et al. investigate the neuronal network at play during memory consolidation in *Drosophila*. They functionally characterize a feedback circuit between dopaminergic and GABAergic neurons that involves two antagonist dopamine receptors and a metabotropic GABA receptor. This circuit regulates olfactory long-term memory formation.

CellPress

Current Biology

Article

CellPress

A GABAergic Feedback Shapes Dopaminergic Input on the *Drosophila* Mushroom Body to Promote Appetitive Long-Term Memory

Alice Pavlowsky,[1] Johann Schor,[1] Pierre-Yves Plaçais,[1] and Thomas Preat[1,2,*]
[1]Genes and Dynamics of Memory Systems, Brain Plasticity Unit, CNRS, ESPCI Paris, PSL Research University, 10 rue Vauquelin, 75005 Paris, France
[2]Lead Contact
*Correspondence: thomas.preat@espci.fr
https://doi.org/10.1016/j.cub.2018.04.040

SUMMARY

Memory consolidation is a crucial step for long-term memory (LTM) storage. However, we still lack a clear picture of how memory consolidation is regulated at the neuronal circuit level. Here, we took advantage of the well-described anatomy of the *Drosophila* olfactory memory center, the mushroom body (MB), to address this question in the context of appetitive LTM. The MB lobes, which are made by the fascicled axons of the MB intrinsic neurons, are organized into discrete anatomical modules, each covered by the terminals of a defined type of dopaminergic neuron (DAN) and the dendrites of a corresponding type of MB output neuron (MBON). We previously revealed the essential role of one DAN, the MP1 neuron, in the formation of appetitive LTM. The MP1 neuron is anatomically matched to the GABAergic MBON MVP2, which has been attributed feedforward inhibitory functions recently. Here, we used behavior experiments and *in vivo* imaging to challenge the existence of MP1-MVP2 synapses and investigate their role in appetitive LTM consolidation. We show that MP1 and MVP2 neurons form an anatomically and functionally recurrent circuit, which features a feedback inhibition that regulates consolidation of appetitive memory. This circuit involves two opposite type 1 and type 2 dopamine receptors in MVP2 neurons and the metabotropic GABA$_B$-R1 receptor in MP1 neurons. We propose that this dual-receptor feedback supports a bidirectional self-regulation of MP1 input to the MB. This mechanism displays striking similarities with the mammalian reward system, in which modulation of the dopaminergic signal is primarily assigned to inhibitory neurons.

INTRODUCTION

Formation of a memory engram is a multi-step process, from encoding the relevant information to the final storage of memory traces [1, 2]. Describing the neuronal architecture and functions that underlie each step of this process is crucial to understanding memory ability. In *Drosophila*, we now have a very fine knowledge of the anatomy of the mushroom body (MB), the major olfactory integrative brain center, as well as its input and output neurons [3, 4]. The mapping to these circuits of various functional modalities occurring at the different stages of memory encoding, storage, and recall is also quite advanced [5–13].

Drosophila MBs are paired structures including ∼2,000 intrinsic neurons per brain hemisphere. These neurons receive dendritic input from the antennal lobes through projection neurons in the calyx area on the posterior part of the brain. Their axons form a fascicle, called a peduncle, that traverses the brain to the anterior part, where axons branch to form horizontal and vertical lobes according to three major branching patterns (α/β, α'/β' and γ). MB lobes are tiled by spatially segregated presynaptic projections from dopamine neurons (DANs), on the one hand, and dendrites of MB output neurons (MBONs), on the other hand [3]. DANs and MBONs are matched to form defined anatomical compartments that are increasingly considered as independent functional units. On several of these compartments, it was shown that DAN activity can induce heterosynaptic plasticity at the MB/MBON synapse, which could be a cellular substrate of memory encoding [11, 14–16].

In addition to this canonical anatomical motif of the DAN/MB intrinsic neurons/MBON triad, electron microscopy connectome reconstruction in the larval brain has evidenced recently that DANs have direct synaptic connections to their matched MBONs [17]. In the adult, direct DAN-to-MBON synapses have also been observed in several compartments of the MB vertical lobes [18].

MB activity is regulated by a broad spectrum of neuromodulatory input, among which tonic dopamine signaling plays an important role in the regulation of memory persistence [12, 19–21] or expression [9]. In particular, we showed that sustained rhythmic activity of the MP1 DAN, also named PPL1-γ1pedc [3] and which innervates the γ1 module and the α/β peduncle, is crucial after conditioning to enable the consolidation of both aversive [12, 22] and appetitive [20] long-term memory (LTM), the most stable memory forms that rely on *de novo* protein synthesis [23–25]. The MP1 neuron is anatomically matched with the MVP2 neuron, a GABAergic MBON that shows a complex arborization. The MVP2 neuron, also named MBON-γ1pedc > α/β [3], possesses two dendritic domains on the γ1 and peduncle compartments [3, 26]. On the ipsilateral

CellPress

side, MVP2 has presynaptic projections on MB vertical and medial lobes and also targets brain areas outside MB where other MBONs project. In particular, MVP2 neurons mediates a feedforward inhibition of specific MBONs involved in aversive and appetitive memory retrieval [26]. Interestingly, MVP2 neurons also send a presynaptic projection onto the contralateral peduncle [3, 26], a place of MP1 presynaptic coverage. Hence, the anatomy of the MP1-MVP2 neurons is compatible with the existence of feedback circuitry. Here, we tested experimentally the existence of such a functional feedback in the context of appetitive LTM formation.

Appetitive memory results from the paired delivery of an odorant and a sugar to starved flies [27]. Only one pairing is sufficient to form both short-term memory (STM) and LTM [23, 24], but it was shown that these two memory phases stem from distinct properties of the reinforcing sugar: although the sweetness of the sugar is sufficient so that flies form appetitive STM, the formation of LTM requires that the conditioning is made with a caloric sugar [28]. The nutritional value of the reinforcing sugar translates in the fly brain as a post-ingestive sustained rhythmic signaling from MP1 neurons that is necessary to consolidate LTM [20]. At the cellular level, STM and LTM stem from parallel and independent memory traces located in distinct subsets of MB neurons; respectively, γ neurons and α/β neurons [29]. Several MB output circuits have been involved in the retrieval of appetitive STM (MBON-$\gamma 2\alpha$'1 [8]), LTM (MBON-$\alpha 3$, MBON-$\alpha 1$ [19, 30]), or both (M4/M6, also named MBON-$\gamma 5\beta$'2a/MBON-β'2mp [11]), providing as many candidate synaptic sites of memory encoding.

In this work, we confirm that post-training MP1 activity is required for LTM formation, but we show in addition that this activity must be temporally restricted. We demonstrate that MP1 activity is self-regulated through an inhibitory feedback by MVP2 neurons. Immediately after conditioning, the oscillatory activity of MP1 is enhanced and MVP2 is inhibited. After about 30 min, MVP2 is activated, terminating the period of MP1 increased signaling, which, we show, is a requirement for proper LTM formation. We propose that the bidirectional action of this feedback loop is based at the molecular level on the sequential involvement of two antagonist dopamine receptors, the type 1 DAMB and the type 2 dD2R on one side and the metabotropic GABA$_B$-R1 receptor on the other side.

RESULTS

Two Antagonist Dopamine Receptors Are Required in MVP2 Neurons for Appetitive Memory

Appetitive olfactory LTM is encoded in the α/β neurons [19, 29]. We induced appetitive olfactory LTM by using a previously described paradigm in which flies that had been starved for 21 hr are first exposed to an odorant while they have access to sucrose, followed by a second odorant without sucrose presentation [23, 24].

In order to specifically investigate the direct connection between MP1 and MVP2 neurons without globally affecting the physiology of the whole MB compartment, we expressed RNAi against dopamine receptors in MVP2. Four dopamine receptors have been characterized in *Drosophila*. dDA1 is the homolog of mammalian D1 receptor. DAMB (dopamine receptor in MB)

was originally described as another type 1 receptor, because it can be positively coupled to cyclic AMP (cAMP) [31, 32] signaling, although it can also trigger calcium signaling [31, 33] through Gq coupling [34]. Sequence comparisons revealed that it rather belongs to an "invertebrate type" class of dopamine receptors [35]. Both dDA1 and DAMB are necessary in the MB for appetitive olfactory memory [19, 20]. dD2R is the homolog of the mammalian D2 receptor and has an inhibitory effect on downstream cAMP signaling [35]. Finally, DopEcR is a dual ecdysone and dopamine receptor, which is also a type 1 dopamine receptor with no clear homology to mammalian receptors [36].

We first downregulated DAMB in MVP2 neurons by expressing a RNAi against DAMB under the control of the highly specific MVP2 split-Gal4 driver *MB112C* [3]. Under these conditions, we observed an appetitive LTM defect, whereas memory retention after 2 hr (hereinafter termed 2-hr memory), olfactory acuity, and sugar response were all normal (Figures 1A and 1B; Table S1). We obtained the same results using a second non-overlapping DAMB RNAi (Figures S1A and S1B; Table S1). To exclude any developmental effect from DAMB RNAi expression, we used the *R83A12* MVP2 Gal4 driver [26, 37] in combination with the thermosensitive Gal4 inhibitor Gal80ts expressed ubiquitously (*tubulin-Gal80^{ts}*) [38]. Restricting the downregulation of DAMB in MVP2 neurons to the adult stage still resulted in an LTM impairment (Figure 1C) without any effect on 2-hr memory (Figure 1D). Without thermal induction, LTM was normal, and so were the sugar response and olfactory acuity (Figure S1C; Table S1). In contrast to DAMB, a knockdown in MVP2 neurons of the two other D1-like receptors, dDA1 and DopEcR, did not affect LTM (Figures S1D and S1E). Hence, DAMB seems to be the only type 1 receptor mediating dopaminergic input on MVP2 for appetitive LTM.

We next addressed the question of the D2-like receptor requirement in MVP2 for appetitive LTM. Intriguingly, we observed also an LTM defect when dD2R was constitutively downregulated in MVP2 using the *MB112C* split-Gal4 driver (Figure 1E). However, 2-hr memory was also affected by dD2R constitutive downregulation in MVP2m whereas olfactory acuity and sugar response were all normal (Figure 1F; Table S1). To exclude any developmental effect from dD2R RNAi expression, we restricted the downregulation of dD2R in MVP2 neurons to the adult stage using only the *tubulin-Gal80^{ts}; R83A12-Gal4*. Similarly to the constitutive downregulation, both LTM and 2-hr memory were impaired (Figures 1G and 1H), while sugar response and olfactory acuity were normal (Table S1). Without induction of the RNAi, LTM performance was normal (Figure S1F).

These results, altogether, indicate that dopamine signaling acts on MVP2 neurons for appetitive memory. Surprisingly, two dopamine receptors with opposite effects on downstream signaling are involved in the formation of appetitive LTM. MVP2 dendrites are intertwined with MP1 terminals in the $\gamma 1$ and peduncle MB modules. In addition, in the electron microscopy reconstruction of the adult MB vertical lobes, no synapses were found between other DANs and MVP2 neurons in which MVP2 is post-synaptic (Table 5 in [18]). Hence, dopaminergic input on MVP2 is likely to come from MP1 neurons. To understand this phenomenon, we therefore focused on the temporal involvement of both MP1 and MVP2 neurons.
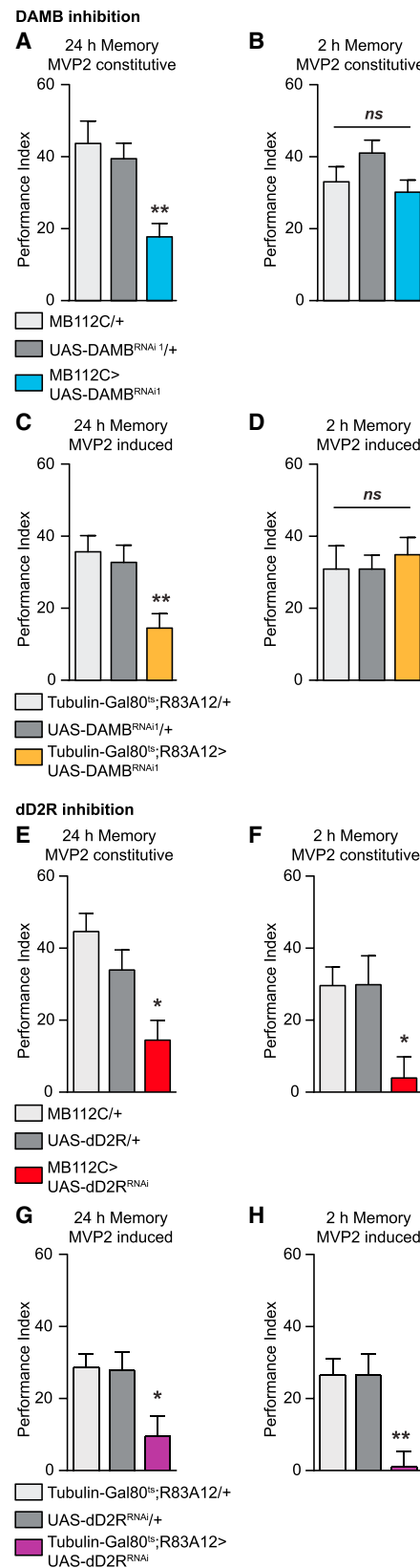
DAMB inhibition

A 24 h Memory MVP2 constitutive

B 2 h Memory MVP2 constitutive

MB112C/+
UAS-DAMB^RNAi 1/+
MB112C> UAS-DAMB^RNAi1

C 24 h Memory MVP2 induced

D 2 h Memory MVP2 induced

Tubulin-Gal80^ts;R83A12/+
UAS-DAMB^RNAi1/+
Tubulin-Gal80^ts;R83A12> UAS-DAMB^RNAi1

dD2R inhibition

E 24 h Memory MVP2 constitutive

F 2 h Memory MVP2 constitutive

MB112C/+
UAS-dD2R/+
MB112C> UAS-dD2R^RNAi

G 24 h Memory MVP2 induced

H 2 h Memory MVP2 induced

Tubulin-Gal80^ts;R83A12/+
UAS-dD2R^RNAi/+
Tubulin-Gal80^ts;R83A12> UAS-dD2R^RNAi

Figure 1. Dopaminergic Signaling Is Required in MVP2 Neurons for Appetitive LTM

(A and B) In (A), constitutive downregulation of DAMB in MVP2 neurons impaired appetitive LTM (n = 16), $F_{(2, 45)}$ = 9.25, $p < 0.001$; whereas in (B), constitutive downregulation of DAMB in MVP2 neurons did not affect 2-hr memory (n = 14), $F_{(2, 39)}$ = 0.69, $p = 0.51$. Similar results were observed using a second non-overlapping DAMB RNAi (see Figures S1A and S1B). Inhibition of any of the other D1-like dopamine receptors (dDA1 and DopEcR) in MVP2 did not affect LTM (see Figures S1C and S1D).

(C and D) In (C), downregulation of DAMB in MVP2 adult neurons impaired LTM (n = 10), $F_{(2, 27)}$ = 6.67, $p < 0.005$; whereas non-induced controls displayed normal LTM (see Figure S1C). (D) Downregulation of DAMB in MVP2 adult neurons did not affect 2-hr memory (n = 12), $F_{(2, 33)}$ = 0.20, $p = 0.82$.

(E and F) In (E), constitutive downregulation of the D2-like dopaminergic receptor dD2R in MVP2 neurons impaired appetitive LTM (n = 16), $F_{(2, 45)}$ = 8.07, $p < 0.01$. However, unlike DAMB, dD2R downregulation also impaired 2-hr memory, as shown in (F) (n = 11), $F_{(2, 30)}$ = 5.30, $p < 0.05$.

(G and H) In (G), downregulation of dD2R in MVP2 adult neurons impaired LTM (n = 17), $F_{(2, 49)}$ = 4.87, $p < 0.05$; whereas non-induced controls displayed normal LTM (see Figure S1F). (H) Downregulation of dD2R in MVP2 adult neurons affected 2-hr memory (n = 18), $F_{(2, 51)}$ = 8.74, $p < 0.001$.

Error bars indicate mean ± SEM. Statistical tests were performed using one-way ANOVA. *$p < 0.05$; **$p < 0.01$, in post hoc comparison; ns, not significant. See Table S1 for sugar perception and olfactory acuity controls.

The Effect of MVP2 Activity on LTM Consolidation Is Time Dependent

Since MP1 neurons are required for appetitive LTM consolidation immediately after training [20], and since an activating dopamine receptor is required in MVP2 neurons for proper LTM performance, we wondered whether MVP2 neuronal activity is also required in the first hours of LTM consolidation. To test this hypothesis, we specifically blocked MVP2 neurotransmission by expressing the dominant-negative thermosensitive Shibire protein (Shi^ts) [39] in MVP2 neurons. Using the *MB112C* split-Gal4 driver, we observed that MVP2 blockade for 1.5 hr immediately after appetitive training resulted in a strong LTM impairment (Figure S2A), whereas LTM was normal when the experiment was led at the permissive temperature (Figure S2B). Importantly blocking MVP2 neurons on a later time window, from 1.5 to 3 hr post-conditioning, had no effect on LTM (Figure S2C). Finally, blocking MVP2 neurons immediately after conditioning did not affect 2-hr-memory scores (Figure S2D). The specific requirement of MVP2 neurons' activity after conditioning for LTM, but not for STM, was confirmed using the *R83A12* driver (Figures S2F–S2H).

We previously described the existence of a 0.5-hr time window during which calcium oscillation of MP1 neurons is crucial for LTM consolidation [20]. We thus further refined the analysis of MVP2 requirement over time to ask whether it has the same requirement of MP1 neurons. We first observed that blocking MVP2 neurons for 1 hr after conditioning was sufficient to impair LTM formation (Figure S2E). Strikingly, blocking MVP2 neurons immediately after conditioning for 0.5 hr did not impair LTM (Figure 2A), while blocking between 0.5 hr and 1 hr post-conditioning did (Figure 2B). Hence, the requirement of MVP2 for appetitive LTM starts at the end of the time period of MP1 neuron's requirement.

In a recent report, it was shown that suppressing the activity of MVP2 neurons during an odor presentation leads to the formation of an aversive memory toward this odor [40]. This raises the question of whether the defect in appetitive LTM that we observed in this series of experiments is due to the blockade
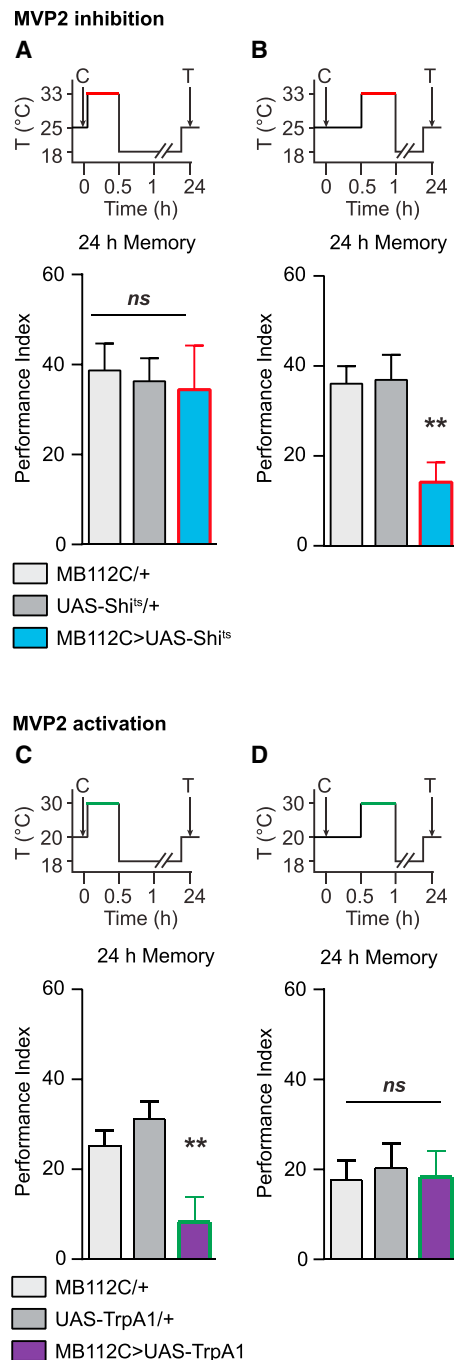
CellPress

MVP2 inhibition

MVP2 activation

Figure 2. MVP2 Activity Is Necessary for Appetitive LTM Formation

(A and B) In (A), MVP2 inhibition from 0 to 0.5 hr did not affect LTM (n = 12), $F_{(2, 33)} = 0.09$, p = 0.92; whereas in (B), MVP2 inhibition from 0.5 to 1 hr impaired LTM (n = 18), $F_{(2, 51)} = 7.58$, p < 0.01. As expected, blocking MVP2 output for the period including the 0.5- to 1-hr period post-conditioning impaired LTM, whereas LTM was normal at a permissive temperature as well as when MVP2 output was blocked 1.5 hr after conditioning (see Figures S2A–S2D). When MVP2 output was blocked immediately after conditioning, 2-hr memory was normal (see Figure S2E).

(C and D) In (C), MVP2 activation from 0 to 0.5 hr impaired LTM (n = 18), $F_{(2, 51)} = 7.30$, p < 0.01; whereas in (D), MVP2 activation from 0.5 to 1 hr did not affect LTM (n = 12), $F_{(2, 33)} = 0.08$, p = 0.93.

of an actual role of MVP2 neurons in memory consolidation or to the fact that MVP2 silencing behaves like an aversive learning signal. However, in favor of the former alternative, we observed that the appetitive LTM of wild-type flies was not sensitive to the delivery of a series of electric shocks 45 min after conditioning, i.e., in the middle of the time window when MVP2 silencing gives an appetitive LTM defect (Figure S2I). Overall, we conclude that the activity of MVP2 neurons is actually required after appetitive conditioning for LTM formation.

The dD2 receptor is required in MVP2 neurons for LTM formation, which suggests that MVP2 neurons have to be inhibited at some point by dopamine signaling. To test this hypothesis, we expressed the thermosensitive cation channel TrpA1 with *MB112C* to allow for temperature-induced overactivation of MVP2 neurons. When MVP2 neurons were activated immediately after conditioning for 0.5 hr, LTM performance was impaired (Figure 2C). By contrast, overactivation of MVP2 neurons between 0.5 hr and 1 hr post-conditioning did not alter LTM (Figure 2D), consistent with MVP2 activity being necessary during this time window (Figure 2B).
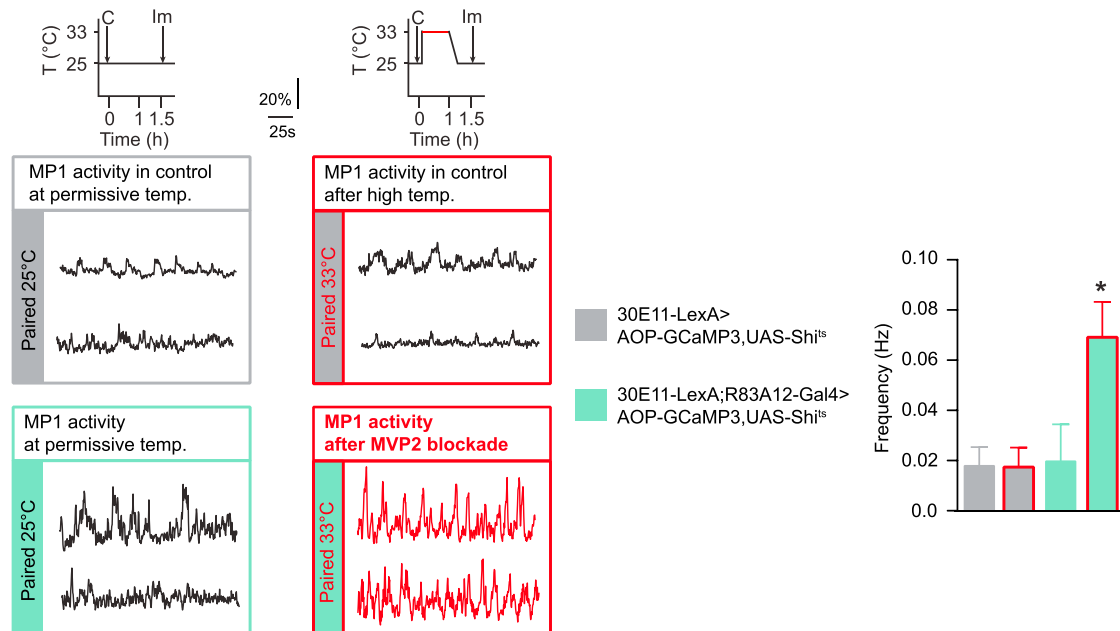
These results indicate that MVP2 neurons are involved in LTM formation according to a precise timing. Activity from MVP2 is deleterious for LTM immediately after conditioning but beneficial from 0.5 hr post-conditioning. Strikingly, the time interval where MVP2 activation is deleterious precisely matches the period when MP1 neurons need to be active. This prompted us to investigate whether MVP2 neurons could inhibit MP1 activity. We first sought to gather anatomical clues in support of this hypothesis. We could observe a co-labeling of MVP2 pre-synaptic boutons labeled with hemagglutinin (HA)-tagged synaptotagmin and of MP1 neurons labeled with membrane-bound GFP. This confirms the presence of MVP2 pre-synaptic connections in the α/β peduncle compartment at the site of MP1 dendritic arborization (Figures S2I and S2J), as suggested by Aso et al. [3]. Hence, anatomical data indicate that the MVP2 neuron can, indeed, directly give feedback to the MP1 neuron to modulate its activity.

MVP2 Neurons Are Required to Terminate the Enhanced Oscillation Period in MP1 Neurons after Appetitive Training
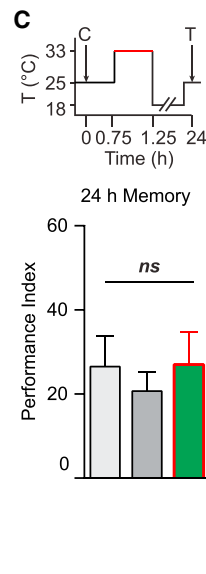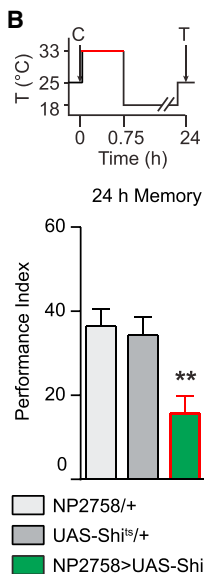
The association of an odor and a sugar leads to a robust appetitive LTM only if the sugar carries a nutritious value [28]. Previously, we showed that the pairing of an energetic sugar with an odorant increased the frequency of MP1 calcium oscillations, as compared to pairing with a non-energetic sugar [20]. Here, we monitored MP1 calcium activity by expressing the GCaMP3 probe in MP1 neurons using the *LexA/LexAop* system [41, 42] with the *30e11-LexA* driver [22] to allow for independent manipulation of MVP2 neurons using the *GAL4/UAS* system. In accordance with our previous work, we observed an increase in the frequency of MP1 oscillations when the nutritious sugar presentation was associated with the odorant presentation

Time courses of temperature shifts are displayed above the performance index histograms (C, conditioning; T, test). Red or green periods in the time courses represent when neurotransmission was blocked (Shi[ts] experiments) or activated (TrpA1 experiments), respectively. Error bars indicate mean ± SEM. Statistical tests were performed using one-way ANOVA. **p < 0.01, in post hoc comparison; ns, not significant.
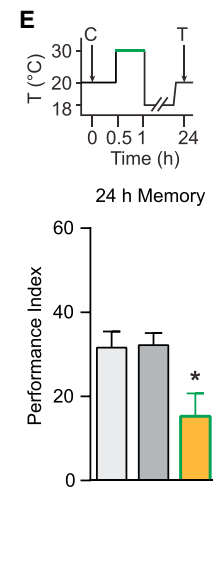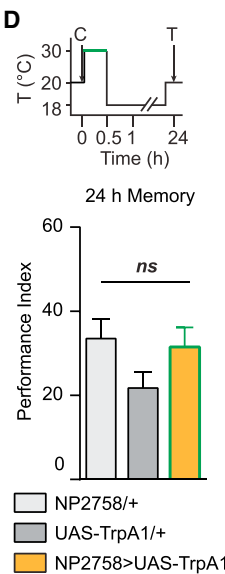
CellPress

Figure 3. MVP2 Modulates MP1 Oscillations after Paired Training

(A) After paired training, flies were stored either at 33°C for 1 hr to block MVP2 neurons or at 25°C for permissive controls; flies were thus imaged 1.5 hr after training. When MVP2 activity was blocked for 1 hr after paired training (*30E11-LexA;R83A12-Gal4 > AOP-GCaMP3;UAS-Shi^{ts}* flies at 33°C), the frequency of MP1 oscillations was significantly higher than in the permissive-temperature condition (paired 25°C, *30E11-LexA;R83A12-Gal4 > AOP-GCaMP3;UAS-Shi^{ts}* flies) and genotype-control condition (paired 33°C, *30E11-LexA;+ > AOP-GCaMP3;UAS-Shi^{ts}* flies) (n = 9), F(3, 32) = 4.83, p < 0.05. Similarly to the oscillations frequency, the quality factor of MP1 calcium oscillation was increased, whereas the amplitude of MP1 calcium oscillations was not significantly affected by paired training or blocking of MVP2 activity (see Figure S3). Control experiments were done immediately after conditioning, using both *30E11-LexA;R83A12-Gal4 > AOP-GCaMP3;UAS-Shi^{ts}* and *30E11-LexA;+ > AOP-GCaMP3;UAS-Shi^{ts}* flies to assess that the association between the odorant and the sugar (paired protocol) induced an increase in both the frequency and the quality factor of MP1 oscillations compared to an unpaired protocol in which the presentation of the sugar is done before odor presentation (see Figure S3). The amplitude of MP1 oscillations was not modified between paired and unpaired protocols (see Figure S3). Illustrative examples of MP1 neuron recordings are displayed for each genotype and condition; controls are indicated in black, and the condition in which MVP2 neuron activity is blocked is indicated in red. Time courses of temperature shifts are displayed above the MP1 recordings. C, conditioning, Im, imaging.

(B and C) In (B), MP1 inhibition immediately after conditioning for 0.75-hr impaired LTM (n = 24), F(2, 71) = 7.24, p < 0.01; whereas in (C), MP1 inhibition from 0.75 hr to 1.25 hr did not affect LTM (n = 12), F(2, 33) = 0.27, p = 0.76.

(legend continued on next page)

(paired protocol), as compared to an unpaired protocol in which the sugar and odorant presentations are dissociated (Figures S3A–S3H). These results further support that the increase in MP1 oscillation frequency observed in paired flies is not merely due to the ingestion of a caloric sugar but is also truly linked to appetitive LTM formation.

To challenge functionally the existence and the physiological significance of an MVP2-to-MP1 feedback, we monitored MP1 neuron activity after blocking MVP2 in flies trained for appetitive memory. Our previous study also demonstrated that the enhanced MP1 oscillations associated with appetitive LTM formation last for less than 1 hr after conditioning. Because MVP2 neurons are inhibitory GABAergic neurons, we hypothesized that their activity might be required to terminate the enhanced MP1 oscillation phase. We used the paired protocol to train flies expressing GCaMP3 in MP1 and Shi^{ts} in MVP2 (*30E11-LexA;R83A12-Gal4 > AOP-GCaMP3 UAS-Shi^{ts}*), as well as their control flies (*30E11-LexA > AOP-GCaMP3 UAS-Shi^{ts}*), which do not express Shi^{ts}. In flies in which MVP2 neurons were blocked for 1 hr after training, we observed prolonged high-frequency oscillations in comparison to the permissive (*30E11-LexA;R83A12-Gal4 > AOP-GCaMP3 UAS-Shi^{ts}* flies at 25°C) and genotypic (*30E11-LexA > AOP-GCaMP3 UAS-Shi^{ts}* flies at 33°C) controls (Figure 3A and S3I–S3L). Behavioral experiments showed that MVP2 neurons are specifically required from 0.5 hr to 1 hr after conditioning (Figure 2). To match the behavioral data, we repeated our imaging experiments but blocking MVP2 neurons only during that time window. In that case, we could still observe an extension of calcium oscillations in MP1 neurons compared to that in genotypic control flies (Figure S3N).

Since blocking MVP2 neurons 0.5 hr after conditioning is detrimental for LTM, these imaging results suggest that the enhancement of MP1 activity, although beneficial immediately after conditioning, needs to be strictly limited in time for proper LTM formation. Indeed, we observed that a delayed blocking of MP1 neurons had no effect on LTM, although blocking MP1 neurons immediately after conditioning impaired LTM as expected (Figures 3B and 3C). Strikingly, activating MP1 neurons for 0.5 hr immediately after conditioning did not impair LTM (Figure 3D), but activating the same neurons from 0.5 hr to 1 hr post-conditioning caused an LTM defect (Figure 3E). These results show that MP1 activity is beneficial for LTM in a limited time window immediately after conditioning but becomes deleterious for LTM afterward. The role of MVP2 neurons in normal conditions is to instruct MP1 neurons to terminate their oscillatory activity at the end of this critical time window.

D-GABA$_B$R$_1$ Mediates GABAergic Input on MP1 Neurons Required for Appetitive LTM and Regulation of MP1 Oscillations
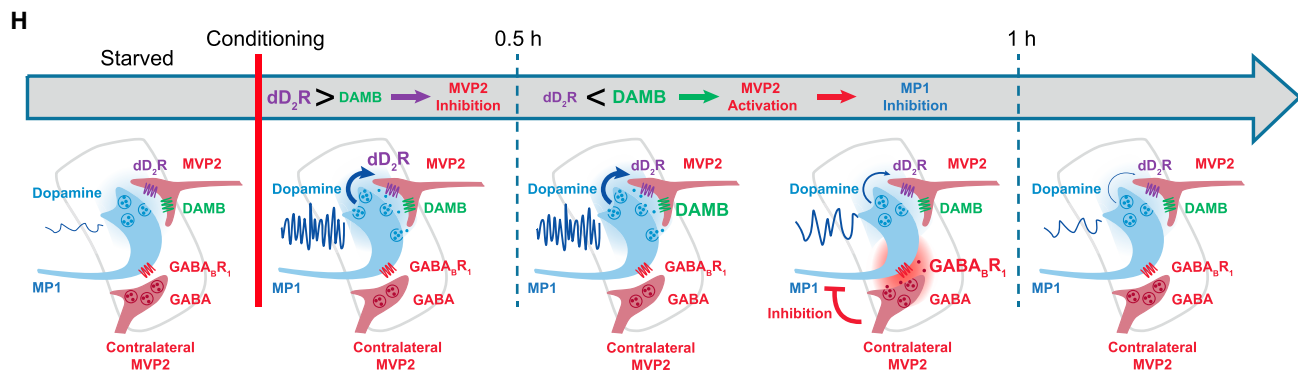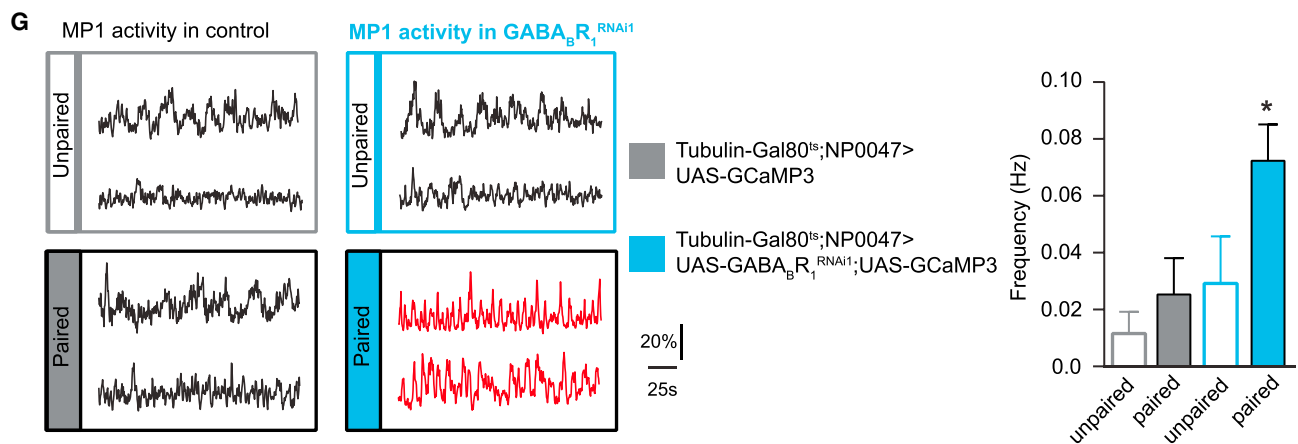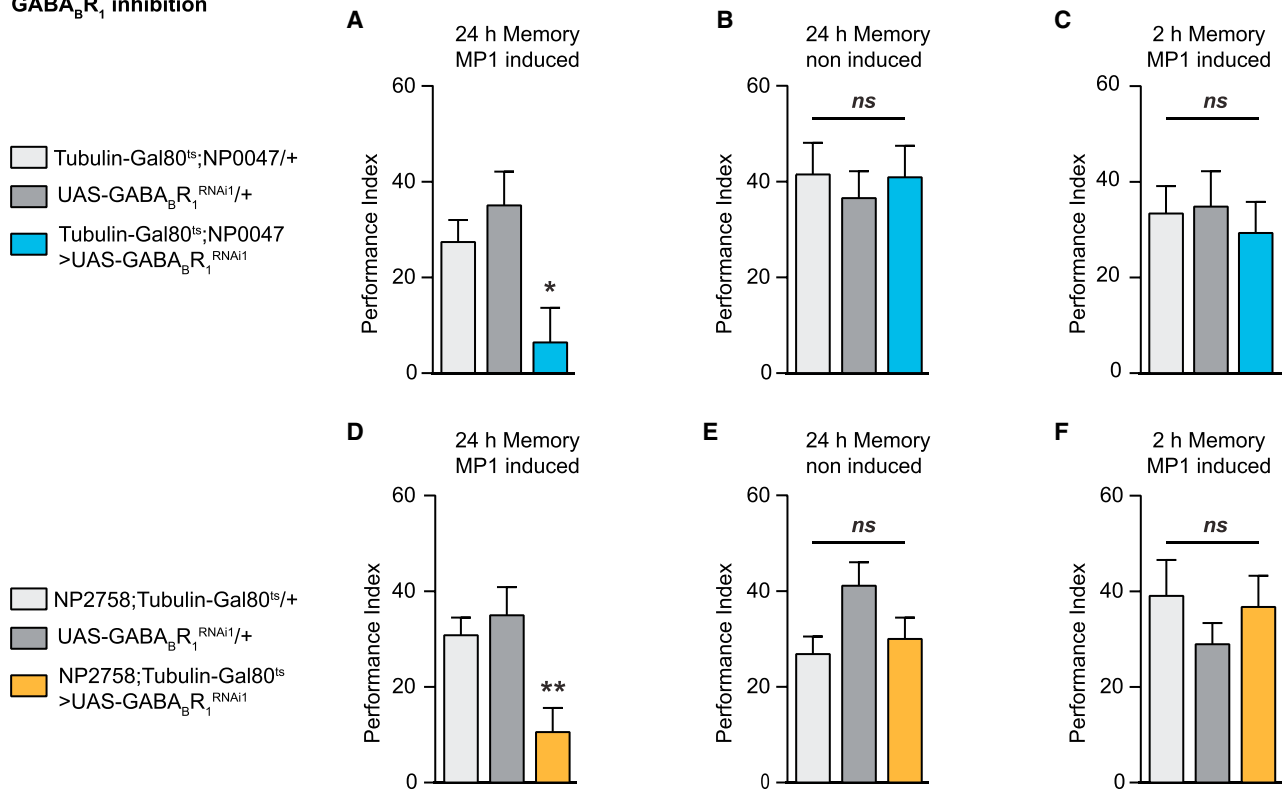
Since MVP2 neurons are GABA-ergic, we asked whether a GABA receptor in MP1 neurons was involved in appetitive LTM formation. Two types of GABA receptors exist in both *Drosophila*

and mammals: ionotropic and metabotropic receptors [43]. Rdl, the main ionotropic receptor, is necessary for appetitive learning in the MB [44]. Three metabotropic GABA receptors have been described in *Drosophila*: D-GABA$_B$R$_1$ and D-GABA$_B$R$_2$, which are highly similar to their mammalian counterparts, and an insect-specific D-GABA$_B$R$_3$. As in mammals, D-GABA$_B$R$_1$ and D-GABA$_B$R$_2$ function as heterodimers, with only D-GABA$_B$R$_1$ binding to GABA [43]. Metabotropic GABA$_B$R are known to be both at the pre- and post-synaptic sites and able to modulate calcium entrance and, consequently, neurotransmitter release at the pre-synaptic site [45, 46]. Therefore, we investigated the potential function of D-GABA$_B$R$_1$ in MP1 neurons. Downregulation of D-GABA$_B$R$_1$ [47] restricted to the adult stage using the *tubulin-Gal80^{ts};NP0047-Gal4* driver—which labels three DANs, including MP1 neurons [12]—induced a strong appetitive LTM impairment (Figure 4A), whereas LTM was normal in non-induced control flies (Figure 4B). Interestingly, 2-hr memory was not affected (Figure 4C), and both sugar response and olfactory acuity were normal (Table S2). These results were reproduced using a second non-overlapping D-GABA$_B$R$_1$ RNAi (Figure S4; Table S2). To confirm the neuron specificity of this effect, we used an inducible *NP2758-Gal4;tubulin-Gal80^{ts}* driver in which the MP1 neurons are the only labeled dopaminergic neurons [9]. Dopaminergic neurons labeled by NP2758-GAL4 are included in those labeled by *NP0047-GAL4* [5]. In these conditions, induced flies exhibited reduced LTM, whereas non-induced flies displayed normal LTM (Figures 4D and 4E). As observed with the other MP1 driver, 2-hr memory was normal in induced flies (Figure 4F), as well as sugar response and olfactory acuity (Table S2). Altogether, our results demonstrate that D-GABA$_B$R$_1$ is required in MP1 neurons for appetitive LTM specifically, and they suggest that these receptors could mediate the MVP2 GABAergic input on MP1 neurons. Since MP1 inputs have not been exhaustively described yet, we cannot completely exclude the existence of other GABAergic inputs to MP1. Our data, therefore, do not necessarily imply that this GABA receptor receives direct input from MVP2 neurons. However, it should be noted that APL, which is the only GABAergic neuron to broadly innervate the MB region, is not required during consolidation for appetitive LTM, whereas it is required for appetitive 3-hr memory [48].

To characterize the effect of GABA on MP1 physiology, we recorded calcium activity in MP1 neurons after training flies expressing (or not expressing) D-GABA$_B$R$_1$ RNAi in MP1 adult neurons. Following downregulation of D-GABA$_B$R$_1$, we observed persistent high-frequency oscillations in MP1 neurons 1.5 hr after the paired training protocol, as compared to either unpaired trained flies expressing the RNAi or paired trained flies in which D-GABA$_B$R$_1$ expression was normal (Figure 4G; Figures S4E–S4M). Thus, either reducing D-GABA$_B$R$_1$ expression in MP1 neurons or blocking MVP2 GABAergic neurons induced persistent high-frequency oscillations in MP1 neurons 1.5 hr after appetitive conditioning, corresponding to a time when oscillations

---

(D and E) In (D), MP1 activation immediately after conditioning for 0.5 hr did not affect LTM (n = 18), $F_{(2, 51)} = 2.01$, p = 0.14; whereas in (E), MP1 activation from 0.5 hr to 1 hr after conditioning impaired LTM (n = 16), $F_{(2, 45)} = 5.26$, p < 0.01. LTM at the permissive temperature was normal (see Figure S3M). Time courses of temperature shifts are displayed above the performance index histograms. (C, conditioning; T, test). Red or green periods in the time courses represent when neurotransmission was blocked (Shi^{ts} experiments) or activated (TrpA1 experiments), respectively.

Error bars indicate mean ± SEM. Statistical tests were performed using one-way ANOVA. *p < 0.05; **p < 0.01, in post hoc comparison; ns, not significant.

CellPress

GABA$_B$R$_1$ inhibition

(legend on next page)

should be back to a normal low-frequency rate. These results, which resemble those obtained with MVP2 blockade (Figure 3), suggest that D-GABA$_B$R$_1$ mediates the action of MVP2 input on MP1 neurons and regulates the frequency of MP1 oscillations. At the presynaptic site, GABA$_B$R$_1$ regulates calcium concentration through either voltage-gated calcium channels or the cAMP pathway [45, 46]. Thus, even if the molecular mechanisms supporting MP1 calcium oscillations remain unknown, the intracellular signaling cascade downstream of D-GABA$_B$R$_1$ that regulates MP1 oscillations is likely to involve one or both of these pathways.

DISCUSSION

In this work we describe a functional inhibitory feedback from an MBON, the GABA-ergic MVP2 neuron, to the dopaminergic neuron of the same MB module, the MP1 neuron. Anatomical data from synaptic staining and electron microscopy, as well as the requirement of a specific GABA receptor in MP1 neurons for appetitive LTM, lead us to favor the hypothesis of a direct connection between MVP2 and MP1 neurons, although alternative scenarios featuring plurisynaptic circuits involving additional GABAergic neurons cannot be ruled out at this stage. Using time-resolved manipulation of neuronal activity, we showed that this feedback circuit is involved in the first hour after appetitive conditioning for LTM formation. It was already known, and we confirmed here, that the activity of MP1 neurons, in the form of regular calcium oscillations, is necessary in the first 30–45 min after conditioning to build LTM [20]. Strikingly, in the present work, we show that, after this initial time period, the activity of MP1 neurons is not merely dispensable but rather deleterious for LTM formation, since activating MP1 neurons from 0.5 hr to 1 hr after conditioning caused an LTM defect.

Conversely, we found that, in that time interval where MP1 neuron activity is deleterious, MVP2 neurons need to be active for normal LTM performance. Imaging experiments showed that blocking MVP2 neurons increased the persistence of MP1 neuron oscillations, up to more than 1 hr post-conditioning. The same effect was observed when the GABAB-R1 receptor was knocked down in MP1 neurons. Interestingly, blocking MVP2 neurons or GABA-ergic signaling in MP1 neurons mostly

affected the frequency and the regularity of MP1 calcium signals, without markedly increasing their amplitude. Hence MVP2 neurons seem to be involved in terminating the period of sustained oscillatory signaling from MP1 neurons rather than merely decreasing MP1 activity. However, in the first 0.5 hr after conditioning, MVP2 neuron activity is not simply dispensable but also deleterious for LTM. Since MVP2 neurons have an inhibitory effect on MP1 activity, it is likely that MVP2 neurons have to be inhibited to let MP1 oscillations occur. Strikingly, we established that MVP2 neurons are modulated by dopamine signaling through two receptors: DAMB, a type 1 activating receptor; and dD2R, a type 2 inhibitory receptor. Although these two receptors have opposite downstream effects, both are required in MVP2 for normal LTM performance.

Overall, our results evidence that the MP1-MVP2 feedback circuit is functionally designed to allow the onset of LTM-gating oscillations only on a precise time windows of about 0.5 hr after conditioning.

We propose that MP1 activity is self-regulated through a dual receptor mechanism that controls MVP2 feedback (Figure 4H). Initially, the ongoing activity of MP1 neurons inhibits MVP2 neurons through the dD2 receptor, which allows for sustained MP1 activity. In a second step, DAMB is activated in MVP2 neurons to enable the inhibitory feedback that shuts off MP1 oscillations. This model unifies our molecular data and the results obtained from time-resolved thermogenetic manipulation of neuronal activity; unfortunately, such temporality of receptor involvement cannot be tested with RNAi-based knockdown.

DAMB and dD2R are two G-protein-coupled dopamine receptors. Although dD2R is a clear homolog of mammalian D2 receptor, and is negatively coupled to cAMP synthesis, the molecular mechanisms downstream of DAMB appear to be more diverse. It was shown that DAMB activation can stimulate cAMP synthesis, similarly to the function of a type 1 receptor [31, 32], likely through G$_{\beta\gamma}$-coupled signaling [49]. Surprisingly, it was recently shown that DAMB-mediated dopamine signaling could transiently inhibit the spiking of sleep-promoting neurons through the same G-protein pathway [50]. Additionally, it was shown that DAMB can also activate downstream calcium signaling from intracellular calcium stores [31, 33, 34]. In our model, MVP2 neurons need, at one point, to be activated to

Figure 4. D-GABA$_B$R$_1$ Downregulation in MP1 Impairs Appetitive LTM and Induces Persistent MP1 Oscillations after Training

(A and B) In (A), knockdown of D-GABA$_B$R$_1$ in MP1 adult neurons impaired LTM (n = 9), $F_{(2, 27)} = 5.41$, $p < 0.05$; whereas in (B), the non-induced controls displayed normal LTM (n = 10), $F_{(2, 29)} = 0.19$, $p = 0.83$.

(C) Expression of D-GABA$_B$R$_1$ RNAi in MP1 adult neurons did not impair 2-hr memory (n = 12), $F_{(2, 33)} = 0.19$, $p = 0.83$. Similar results were observed using a second non-overlapping D-GABA$_B$R$_1$ RNAi (see Figure S4).

(D and E) In (D), LTM was also impaired when a second MP1 inducible driver (NP2758;Tubulin-Gal80^{ts}) was used to downregulate D-GABA$_B$R$_1$ at the adult stage (n = 12), $F_{(2, 33)} = 6.94$, $p < 0.05$; whereas in (E), LTM was normal in non-induced controls (n = 12), $F_{(2, 33)} = 2.93$, $p = 0.07$.

(F) Inhibition of D-GABA$_B$R$_1$ using this second MP1 inducible driver did not affect 2-hr memory (n = 11), $F_{(2, 30)} = 0.71$, $p = 0.50$. See Table S2 for sugar perception and olfactory acuity controls.

(G) The frequency of MP1 calcium oscillations was significantly higher 1.5 hr after appetitive training in flies co-expressing D-GABA$_B$R$_1$ RNAi and GCamP3 in adult MP1 neurons than in unpaired controls and both paired and unpaired flies that do not express the D-GABA$_B$R$_1$ RNAi (n = 9), $F_{(3, 32)} = 4.25$, $p < 0.05$. Illustrative examples of MP1 neuron recordings are displayed for each genotype and condition; controls are indicated in black, and the condition in which paired trained flies express D-GABA$_B$R$_1$ RNAi in MP1 neurons is indicated in red. Similarly to the oscillations frequency, the quality factor of MP1 calcium oscillation was increased, whereas the amplitude of MP1 calcium oscillations was not affected (see Figures S4D and S4E). Control imaging experiments using the other odorant used for behavior experiment (methylcyclohexanol) were done to assess that the effect of inhibiting metabotropic GABA signalization in MP1 is not odorant specific (see Figures S4I–S4M).

(H) Schematic depicting how the MP1 and MVP2 neurons regulate their activity over LTM formation. The different metabotropic receptors involved in this feedback loop are represented, and the peduncle area is represented by the light gray outlines.

Error bars indicate mean ± SEM. Statistical tests were performed using one-way ANOVA. *p < 0.05; **p < 0.01, in post hoc comparison; ns, not significant.

dampen MP1 oscillations, so activating functions of DAMB seem to be more relevant in the present environment. Interestingly, physiological measurements in a heterologous system [49] showed that cAMP activation occurs within tens of minutes, while calcium activation occurs on much shorter timescales. The delayed requirement of MVP2 activity (starting ~30 min after conditioning) seems to be more consistent with an activation of the cAMP pathway. It would be helpful in the future to decipher the molecular mechanism downstream of DAMB involved in this feedback loop. The sequential activation of two distinct dopamine receptors could be due to different affinities for dopamine. Indeed, pharmacological studies show that D2R-like receptors have a higher affinity toward dopamine compared to the D1-like receptors in mammals [51]. However, in the specific case of *Drosophila* D2R and DAMB, similar dopamine affinities for both receptors were reported (0.5 μM for D2R [52] and 0.1–1 μM for DAMB [31, 32]), although these are all obtained from *in vitro* preparations of cultured cells. There could be also be subtler differences of activation kinetics based both on the quantity and on the mode of dopamine release by MP1 neurons.

MP1 neurons and MVP2 neurons have been shown to play crucial roles in both aversive and appetitive memories. During aversive conditioning, MP1 neurons mediate the unconditioned stimulus [5], which is thought to involve dDA1 activation in MB neurons [53]. In a recent report, it was shown that suppressing the activity of MVP2 neurons during an odor presentation leads to the formation of an aversive memory toward this odor [40]. In light of this result, these authors proposed that the role of steady-state MVP2 activity is to prevent the formation of irrelevant memory from insignificant stimuli. Given the role of MP1 in the signaling of negative stimuli during aversive learning, this finding and its interpretation are fully consistent with the existence of an inhibitory feedback from MVP2 neurons to MP1 neurons, as reported in the present work. MP1 neurons are also central in the formation of LTM after conditioning. Tonic signaling through slow oscillations of MP1 neurons gates the formation of aversive LTM after spaced training [12, 22]. The same kind of sustained post-training signaling builds LTM after appetitive conditioning ([20], and the present study). Both in aversive and appetitive paradigms, this LTM-gating function involves DAMB signaling in MB neurons. After aversive spaced training, it was shown that DAMB activation triggers an upregulation of MB energy metabolism, which starts the consolidation of LTM [22]. Finally, MP1 neurons also regulate the retrieval of appetitive STM [9]. MP1 inhibition in starved flies, through suppressive dNPF signaling, allows integration of the appetitive motivational state with the expression of MB-encoded memory trace during retrieval to allow for the expression of appetitive STM [9]. This involves enhanced feedforward inhibition from MVP2 neurons to the M4/M6 MBONs [26] that mediate appetitive memory retrieval [11]. The fact that MP1 inhibition goes along with enhanced MVP2 activity is consistent with the fact that baseline MP1 activity can drive an inhibition of MVP2 through dD2R, as we report here. This may explain why a knockdown of dD2R in MVP2 neurons, by indiscriminately disturbing this MP1-MVP2 inhibitory link, would impair the odor-specific message carried by M4/M6 neurons for memory retrieval and cause an STM defect (Figure 1). All these findings

illustrate how the sophistication of MP1 neuron involvement in memory is tightly linked to the diversity of receptors and neuronal targets that it can activate. A finer understanding of these processes calls for higher resolution physiological measurements to understand how the various dopamine receptors are sensitive to different modalities or kinetics of dopamine release.

Recently, it was shown that acquisition and consolidation of appetitive LTM also rely on a positive-feedback circuit involving the α1 MB compartment, dopaminergic PAM-α1, and glutamatergic MBON-α1 neurons [19]. Thus, consolidation of appetitive memory involves two different recurrent circuits that share common features, such as the MBON's dual functions in consolidation and retrieval of memory. MP1 neurons are activated after a conditioning with a nutritious sugar [20], which is necessary for LTM formation [28]. PAM-α1 neurons are activated during conditioning [21, 54] and probably mediate the coincidence detection between sugar intake and odor perception within MB neurons. The recurrent activity of the α1 compartment loop is also necessary for proper LTM formation, presumably to stabilize a nascent memory trace [19]. Interestingly, the electron microscopy reconstruction of the adult MB vertical lobes recently showed that MVP2 neurons form direct synapses with MBONs in the α2 and α3 modules and, probably, in the α1 compartment as well [18]. Therefore, the two feedback circuits may not be independent, and MVP2 neurons may also mediate a feedforward input from the MP1/MVP2 loop to the PAM-α1/MBON-α1 loop. The dD2R-mediated inhibition of MVP2 neurons by MP1 activity immediately after conditioning could, therefore, help in maintaining the recurrent activity in the α1 compartment.

In conclusion, we have shown here that a negative-feedback loop functions to control appetitive LTM formation (Figure 4H), likely involving two antagonist dopaminergic receptors. This negative-feedback loop is strikingly similar to one recently described in the mammalian mesolimbic system in which feedback from inhibitory neurons prevents the over-activation of dopaminergic neurons [55]. These two circuits have at least three common features: they rely on the metabotropic receptors DA1 and $GABA_BR_1$; they comprise dopaminergic and inhibitory neurons, which are monosynaptically connected in mammals, and possibly also in *Drosophila*; and they are involved in the memory acquisition of motivationally relevant stimuli. These shared properties of negative-feedback loops highlight how similar strategies exist at both the network and molecular levels to regulate certain related behaviors across species.

STAR★METHODS

Detailed methods are provided in the online version of this paper and include the following:

- KEY RESOURCES TABLE
- CONTACT FOR REAGENT AND RESOURCE SHARING
- EXPERIMENTAL MODEL AND SUBJECT DETAILS
  - Fly strains
- METHOD DETAILS
  - Behavior Experiments

CellPress

- ○ Temperature-Shift Protocols
- ○ Sugar Response Tests
- ○ Olfactory Acuity
- ○ Immuno-histochemistry experiments
- ○ In Vivo Calcium Imaging
- ○ Quantitative PCR analyses
- ● QUANTIFICATION AND STATISTICAL ANALYSIS

SUPPLEMENTAL INFORMATION

Supplemental Information includes four figures and two tables and can be found with this article online at https://doi.org/10.1016/j.cub.2018.04.040.

AUTHOR CONTRIBUTIONS

Conceptualization, A.P. and T.P.; Investigation, A.P., J.S., and P.-Y.P.; Writing – Original Draft, A.P. and P.-Y.P.; Writing – Review & Editing, A.P., P.-Y.P., & T.P.; Funding Acquisition, T.P.

DECLARATION OF INTERESTS

The authors declare no competing interests.

REFERENCES

1. Dudai, Y., Karni, A., and Born, J. (2015). The consolidation and transformation of memory. Neuron *88*, 20–32.

2. Nader, K., and Hardt, O. (2009). A single standard for memory: the case for reconsolidation. Nat. Rev. Neurosci. *10*, 224–234.

3. Aso, Y., Hattori, D., Yu, Y., Johnston, R.M., Iyer, N.A., Ngo, T.-T.B., Dionne, H., Abbott, L.F., Axel, R., Tanimoto, H., and Rubin, G.M. (2014). The neuronal architecture of the mushroom body provides a logic for associative learning. eLife *3*, e04577.

4. Tanaka, N.K., Tanimoto, H., and Ito, K. (2008). Neuronal assemblies of the *Drosophila* mushroom body. J. Comp. Neurol. *508*, 711–755.

5. Aso, Y., Herb, A., Ogueta, M., Siwanowicz, I., Templier, T., Friedrich, A.B., Ito, K., Scholz, H., and Tanimoto, H. (2012). Three dopamine pathways induce aversive odor memories with different stability. PLoS Genet. *8*, e1002768.

6. Aso, Y., Siwanowicz, I., Bräcker, L., Ito, K., Kitamoto, T., and Tanimoto, H. (2010). Specific dopaminergic neurons for the formation of labile aversive memory. Curr. Biol. *20*, 1445–1451.

7. Claridge-Chang, A., Roorda, R.D., Vrontou, E., Sjulson, L., Li, H., Hirsh, J., and Miesenböck, G. (2009). Writing memories with light-addressable reinforcement circuitry. Cell *139*, 405–415.

8. Felsenberg, J., Barnstedt, O., Cognigni, P., Lin, S., and Waddell, S. (2017). Re-evaluation of learned information in *Drosophila*. Nature *544*, 240–244.

9. Krashes, M.J., DasGupta, S., Vreede, A., White, B., Armstrong, J.D., and Waddell, S. (2009). A neural circuit mechanism integrating motivational state with memory expression in *Drosophila*. Cell *139*, 416–427.

10. Liu, C., Plaçais, P.-Y., Yamagata, N., Pfeiffer, B.D., Aso, Y., Friedrich, A.B., Siwanowicz, I., Rubin, G.M., Preat, T., and Tanimoto, H. (2012). A subset of dopamine neurons signals reward for odour memory in *Drosophila*. Nature *488*, 512–516.

11. Owald, D., Felsenberg, J., Talbot, C.B., Das, G., Perisse, E., Huetteroth, W., and Waddell, S. (2015). Activity of defined mushroom body output neurons underlies learned olfactory behavior in *Drosophila*. Neuron *86*, 417–427.

12. Plaçais, P.-Y., Trannoy, S., Isabel, G., Aso, Y., Siwanowicz, I., Belliart-Guérin, G., Vernier, P., Birman, S., Tanimoto, H., and Preat, T. (2012). Slow oscillations in two pairs of dopaminergic neurons gate long-term memory formation in *Drosophila*. Nat. Neurosci. *15*, 592–599.

13. Séjourné, J., Plaçais, P.-Y., Aso, Y., Siwanowicz, I., Trannoy, S., Thoma, V., Tedjakumala, S.R., Rubin, G.M., Tchénio, P., Ito, K., et al. (2011). Mushroom body efferent neurons responsible for aversive olfactory memory retrieval in *Drosophila*. Nat. Neurosci. *14*, 903–910.

14. Aso, Y., Sitaraman, D., Ichinose, T., Kaun, K.R., Vogt, K., Belliart-Guérin, G., Plaçais, P.-Y., Robie, A.A., Yamagata, N., Schnaitmann, C., et al. (2014). Mushroom body output neurons encode valence and guide memory-based action selection in *Drosophila*. eLife *3*, e04580.

15. Cohn, R., Morantte, I., and Ruta, V. (2015). Coordinated and compartmentalized neuromodulation shapes sensory processing in *Drosophila*. Cell *163*, 1742–1755.

16. Hige, T., Aso, Y., Modi, M.N., Rubin, G.M., and Turner, G.C. (2015). Heterosynaptic plasticity underlies aversive olfactory learning in *Drosophila*. Neuron *88*, 985–998.

17. Eichler, K., Li, F., Litwin-Kumar, A., Park, Y., Andrade, I., Schneider-Mizell, C.M., Saumweber, T., Huser, A., Eschbach, C., Gerber, B., et al. (2017). The complete connectome of a learning and memory centre in an insect brain. Nature *548*, 175–182.

18. Takemura, S.Y., Aso, Y., Hige, T., Wong, A., Lu, Z., Xu, C.S., Rivlin, P.K., Hess, H., Zhao, T., Parag, T., et al. (2017). A connectome of a learning and memory center in the adult *Drosophila* brain. eLife *6*, e26975.

19. Ichinose, T., Aso, Y., Yamagata, N., Abe, A., Rubin, G.M., and Tanimoto, H. (2015). Reward signal in a recurrent circuit drives appetitive long-term memory formation. eLife *4*, e10719.

20. Musso, P.-Y., Tchenio, P., and Preat, T. (2015). Delayed dopamine signaling of energy level builds appetitive long-term memory in *Drosophila*. Cell Rep. *10*, 1023–1031.

21. Yamagata, N., Ichinose, T., Aso, Y., Plaçais, P.-Y., Friedrich, A.B., Sima, R.J., Preat, T., Rubin, G.M., and Tanimoto, H. (2015). Distinct dopamine neurons mediate reward signals for short- and long-term memories. Proc. Natl. Acad. Sci. USA *112*, 578–583.

22. Plaçais, P.-Y., de Tredern, É., Scheunemann, L., Trannoy, S., Goguel, V., Han, K.-A., Isabel, G., and Preat, T. (2017). Upregulated energy metabolism in the Drosophila mushroom body is the trigger for long-term memory. Nat. Commun. *8*, 15510.

23. Colomb, J., Kaiser, L., Chabaud, M.-A., and Preat, T. (2009). Parametric and genetic analysis of *Drosophila* appetitive long-term memory and sugar motivation. Genes Brain Behav. *8*, 407–415.

24. Krashes, M.J., and Waddell, S. (2008). Rapid consolidation to a *radish* and protein synthesis-dependent long-term memory after single-session appetitive olfactory conditioning in *Drosophila*. J. Neurosci. *28*, 3103–3113.

25. Tully, T., Preat, T., Boynton, S.C., and Del Vecchio, M. (1994). Genetic dissection of consolidated memory in Drosophila. Cell *79*, 35–47.

26. Perisse, E., Owald, D., Barnstedt, O., Talbot, C.B., Huetteroth, W., and Waddell, S. (2016). Aversive learning and appetitive motivation toggle feed-forward inhibition in the *Drosophila* mushroom body. Neuron *90*, 1086–1099.

CellPress

27. Tempel, B.L., Bonini, N., Dawson, D.R., and Quinn, W.G. (1983). Reward learning in normal and mutant *Drosophila*. Proc. Natl. Acad. Sci. USA *80*, 1482–1486.

28. Burke, C.J., and Waddell, S. (2011). Remembering nutrient quality of sugar in *Drosophila*. Curr. Biol. *21*, 746–750.

29. Trannoy, S., Redt-Clouet, C., Dura, J.-M., and Preat, T. (2011). Parallel processing of appetitive short- and long-term memories in *Drosophila*. Curr. Biol. *21*, 1647–1653.

30. Plaçais, P.-Y., Trannoy, S., Friedrich, A.B., Tanimoto, H., and Preat, T. (2013). Two pairs of mushroom body efferent neurons are required for appetitive long-term memory retrieval in *Drosophila*. Cell Rep. *5*, 769–780.

31. Feng, G., Hannan, F., Reale, V., Hon, Y.Y., Kousky, C.T., Evans, P.D., and Hall, L.M. (1996). Cloning and functional characterization of a novel dopamine receptor from *Drosophila melanogaster*. J. Neurosci. *16*, 3925–3933.

32. Han, K.A., Millar, N.S., Grotewiel, M.S., and Davis, R.L. (1996). DAMB, a novel dopamine receptor expressed specifically in *Drosophila* mushroom bodies. Neuron *16*, 1127–1135.

33. Cassar, M., Issa, A.-R., Riemensperger, T., Petitgas, C., Rival, T., Coulom, H., Iché-Torres, M., Han, K.-A., and Birman, S. (2015). A dopamine receptor contributes to paraquat-induced neurotoxicity in *Drosophila*. Hum. Mol. Genet. *24*, 197–212.

34. Himmelreich, S., Masuho, I., Berry, J.A., MacMullen, C., Skamangas, N.K., Martemyanov, K.A., and Davis, R.L. (2017). Dopamine receptor DAMB signals via Gq to mediate forgetting in *Drosophila*. Cell Rep. *21*, 2074–2081.

35. Mustard, J.A., Beggs, K.T., and Mercer, A.R. (2005). Molecular biology of the invertebrate dopamine receptors. Arch. Insect Biochem. Physiol. *59*, 103–117.

36. Srivastava, D.P., Yu, E.J., Kennedy, K., Chatwin, H., Reale, V., Hamon, M., Smith, T., and Evans, P.D. (2005). Rapid, nongenomic responses to ecdysteroids and catecholamines mediated by a novel *Drosophila* G-protein-coupled receptor. J. Neurosci. *25*, 6145–6155.

37. Jenett, A., Rubin, G.M., Ngo, T.-T.B., Shepherd, D., Murphy, C., Dionne, H., Pfeiffer, B.D., Cavallaro, A., Hall, D., Jeter, J., et al. (2012). A GAL4-driver line resource for *Drosophila* neurobiology. Cell Rep. *2*, 991–1001.

38. McGuire, S.E., Le, P.T., Osborn, A.J., Matsumoto, K., and Davis, R.L. (2003). Spatiotemporal rescue of memory dysfunction in *Drosophila*. Science *302*, 1765–1768.

39. Kitamoto, T. (2001). Conditional modification of behavior in *Drosophila* by targeted expression of a temperature-sensitive *shibire* allele in defined neurons. J. Neurobiol. *47*, 81–92.

40. Ueoka, Y., Hiroi, M., Abe, T., and Tabata, T. (2017). Suppression of a single pair of mushroom body output neurons in *Drosophila* triggers aversive associations. FEBS Open Bio *7*, 562–576.

41. Lai, S.-L., and Lee, T. (2006). Genetic mosaic with dual binary transcriptional systems in Drosophila. Nat. Neurosci. *9*, 703–709.

42. Pfeiffer, B.D., Truman, J.W., and Rubin, G.M. (2012). Using translational enhancers to increase transgene expression in *Drosophila*. Proc. Natl. Acad. Sci. USA *109*, 6626–6631.

43. Mezler, M., Müller, T., and Raming, K. (2001). Cloning and functional expression of GABA(B) receptors from *Drosophila*. Eur. J. Neurosci. *13*, 477–486.

44. Liu, X., Buchanan, M.E., Han, K.-A., and Davis, R.L. (2009). The GABAA receptor RDL suppresses the conditioned stimulus pathway for olfactory learning. J. Neurosci. *29*, 1573–1579.

45. Bettler, B., Kaupmann, K., Mosbacher, J., and Gassmann, M. (2004). Molecular structure and physiological functions of GABA(B) receptors. Physiol. Rev. *84*, 835–867.

46. Couve, A., Moss, S.J., and Pangalos, M.N. (2000). GABAB receptors: a new paradigm in G protein signaling. Mol. Cell. Neurosci. *16*, 296–312.

47. Yuan, Q., Song, Y., Yang, C.-H., Jan, L.Y., and Jan, Y.N. (2014). Female contact modulates male aggression via a sexually dimorphic GABAergic circuit in *Drosophila*. Nat. Neurosci. *17*, 81–88.

48. Pitman, J.L., Huetteroth, W., Burke, C.J., Krashes, M.J., Lai, S.-L., Lee, T., and Waddell, S. (2011). A pair of inhibitory neurons are required to sustain labile memory in the *Drosophila* mushroom body. Curr. Biol. *21*, 855–861.

49. Reale, V., Hannan, F., Hall, L.M., and Evans, P.D. (1997). Agonist-specific coupling of a cloned *Drosophila melanogaster* D1-like dopamine receptor to multiple second messenger pathways by synthetic agonists. J. Neurosci. *17*, 6545–6553.

50. Pimentel, D., Donlea, J.M., Talbot, C.B., Song, S.M., Thurston, A.J.F., and Miesenböck, G. (2016). Operation of a homeostatic sleep switch. Nature *536*, 333–337.

51. Beaulieu, J.-M., and Gainetdinov, R.R. (2011). The physiology, signaling, and pharmacology of dopamine receptors. Pharmacol. Rev. *63*, 182–217.

52. Hearn, M.G., Ren, Y., McBride, E.W., Reveillaud, I., Beinborn, M., and Kopin, A.S. (2002). A *Drosophila* dopamine 2-like receptor: molecular characterization and identification of multiple alternatively spliced variants. Proc. Natl. Acad. Sci. USA *99*, 14554–14559.

53. Qin, H., Cressy, M., Li, W., Coravos, J.S., Izzi, S.A., and Dubnau, J. (2012). Gamma neurons mediate dopaminergic input during aversive olfactory memory formation in *Drosophila*. Curr. Biol. *22*, 608–614.

54. Huetteroth, W., Perisse, E., Lin, S., Klappenbach, M., Burke, C., and Waddell, S. (2015). Sweet taste and nutrient value subdivide rewarding dopaminergic neurons in *Drosophila*. Curr. Biol. *25*, 751–758.

55. Edwards, N.J., Tejeda, H.A., Pignatelli, M., Zhang, S., McDevitt, R.A., Wu, J., Bass, C.E., Bettler, B., Morales, M., and Bonci, A. (2017). Circuit specificity in the inhibitory architecture of the VTA regulates cocaine-induced behavior. Nat. Neurosci. *20*, 438–448.

56. Turrel, O., Lampin-Saint-Amaux, A., Préat, T., and Goguel, V. (2016). *Drosophila* neprilysins are involved in middle-term and long-term memory. J. Neurosci. *36*, 9535–9546.

STAR★METHODS

KEY RESOURCES TABLE

REAGENT or RESOURCE	SOURCE	IDENTIFIER
Antibodies		
Anti-GFP (rabbit)	Life Technologies	Cat#A11122
Anti-HA (rat)	Roche/Sigma	Cat#11867423001
Anti-nc82 (mouse)	DSHB	Cat# nc82, RRID:AB_2314866
Anti-rat AlexA 594	Life Technologies	Cat#A11007
Anti-rabbit AlexA 488	Life Technologies	Cat#A11034
Anti-mouse AlexA 647	Life Technologies	Cat#A21235
Chemicals, Peptides, and Recombinant Proteins		
4-methylcyclohexanol (98%)	Sigma-Aldrich	Cat#218405
3-octanol (99%)	Sigma-Aldrich	Cat#153095
Paraffine GPR Rectapur	VWR	Cat#24679.360
Bovin Serum Albumin	EuroMedex	Cat#04-100-812-C
PFA	Electron Microscopy Science	Cat#15710
Triton X-100	Sigma-Aldrich	Cat#93443
Prolong Mounting Medium	Life Technologies	Cat#P36965
NaCl	Sigma-Aldrich	Cat#S9625
KCl	Sigma-Aldrich	Cat#P3911
$MgCl_2$	Sigma-Aldrich	Cat#M9272
$CaCl_2$	Sigma-Aldrich	Cat#3881
ribose	Sigma-Aldrich	Cat#W379301
HEPES-NaOH	Sigma-Aldrich	Cat#H7637
Sucrose	Sigma-Aldrich	Cat#S9378
DNaseI	New England Biolabs	Cat#M0303S
Critical Commercial Assays		
RNeasy Plant Mini Kit	QIAGEN	Cat#74904
RNA Minielute Cleanup kit	QIAGEN	Cat#74204
SuperScript III First-Strand kit	Thermofisher Invitrogen	Cat#18080-051
SYBR Green I Master mix	Roche	Cat#04729692001
Experimental Models: Organisms/Strains		
MB112C-split GAL4	[3]	N/A
R83A12-Gal4	BDSC	N/A
30E11-LexA	BDSC	N/A
30E11-LexA;R83A12-Gal4	This paper	N/A
NP2758-GAL4	[20]	N/A
NP0047-Gal4	[12]	N/A
Tubulin-GAL80^{ts} line as described in [20]]	BDSC	N/A
Tubulin-GAL80^{ts};NP0047-Gal4	This paper	N/A
Tubulin-GAL80^{ts};NP2758-Gal4	This paper	N/A
Tubulin-GAL80^{ts};R83A12-Gal4	This paper	N/A
UAS-Shi^{ts}	[12]	N/A
UAS-TrpA1	[12]	N/A
UAS-dDA1^{RNA1} (KK102341)	VDRC	VDRC v107058
UAS-GABA$_B$R$_1^{RNAi1}$ (KK109166)	VDRC	VDRC v101440
UAS-DAMB^{RNAi2} (KK110947)	VDRC	VDRC v105324
UAS-DAMB^{RNAi1} (JF02043)	BDSC	BDSC 26018

(Continued on next page)

Continued

REAGENT or RESOURCE	SOURCE	IDENTIFIER
UAS-DopEcR^RNAi1(KK111211)	VDRC	VDRC v103494
UAS-dD2R^RNAi1 (JF02025)	BDSC	BDSC 26001
UAS-GABA_BR_1^RNAi2 (HMC03388)	BDSC	BDSC 51817
AOP-GCaMP3	Barret Pfeiffer (Janelia Research Center)	N/A
UAS-IVS-GCaMP3 in VK00005	Barret Pfeiffer (Janelia Research Center)	N/A
AOP-GCaMP3, UAS-Shi	This paper	N/A
UAS-GABA_BR_1^RNAi1 (KK109166);UAS-IVS-GCaMP3	This paper	N/A
UAS-Syt-HA;;	Pr. Hiromu Tanimoto (Tohoku University, Japan)	N/A
;;AOP-mCD8::GFP	BDSC	BDSC 32203
UAS-Syt-HA;;AOP-mCD8::GFP	This paper	N/A
Oligonucleotides		
Primer GABA BR1 forward: 5′TTGGATGATGTCAACAAGCAG −3′	This Paper	N/A
Primer GABA B R1 reverse: 5′TTTTGCGGTTTATTATAGAGCAGAT −3′	This Paper	N/A
Primer Tubulin forward: 5′-TTGTCGCGTGTGAAACACTTC-3′	[56]	N/A
Primer Tubulin forward: 5′-CTGGACACCAGCCTGACCAAC-3′	[56]	N/A
Software and Algorithms		
GraphPad Prism 5	GraphPad Software Inc. Press, San Diego CA, 2007	http://www.graphpad.com/
MATLAB V2013	The Mathworks Inc., Natick, MA	https://fr.mathworks.com/
Fiji	NIH	https://imagej.net/Fiji

CONTACT FOR REAGENT AND RESOURCE SHARING

Further information and requests for resources and reagents should be directed to and will be fulfilled by the Lead contact, Thomas Preat (thomas.preat@espci.fr)

EXPERIMENTAL MODEL AND SUBJECT DETAILS

Fly strains

Fly stocks were raised on standard cornmeal food at 18°C and 60% relative humidity under a 12:12 hr light:dark cycle. To express transgenes in MVP2 we used *MB112C-split GAL4* [3] or *R83A12-Gal4* [37]. To express transgenes in MP1 neurons we used either *NP0047-GAL4* [12] or *NP2758-GAL4* [20], or *30E11-LexA* [22]. These lines were used to construct the *30E11-LexA;R83A12-Gal4* line. To restrict UAS/GAL4-mediated expression to the adult stage, we used the TARGET system with the *tubulin-GAL80^ts* line as described in [20]] to construct three new lines: *Tubulin-GAL80^ts;NP0047-Gal4*, *Tubulin-GAL80^ts;NP2758-Gal4* and *Tubulin-GAL80^ts;R83A12-Gal4*. GAL4 activity was released by transferring adult flies to a 30°C incubator for 2 days. The expression pattern of each constructed driver line was checked by immunostaining (data not shown). The *UAS-shi^ts* and the *UAS-TrpA1* lines were previously used in [4]. The following dopamine and GABA receptors RNAi lines came from the Vienna *Drosophila* Resource Center (VDRC): *UAS-dDA1^RNA1* (KK102341, VDRC v107058), *UAS-GABA_BR_1^RNAi1* (KK109166, VDRC v101440) and *UAS-DAMB^RNAi2* (KK110947 VDRC v105324), *UAS-DopEcR^RNAi1* (KK111211 VDRC v103494), whereas the others came from the Transgenic RNAi Project (TRiP): *UAS-DAMB^RNAi1* (JF02043, Bloomington *Drosophila* Stock Center (BDSC) BDSC 26018), *UAS-GABA_BR_1^RNAi2* (HMC03388, BDSC ID51817), *UAS-dD2R^RNAi1*(JF02025, BDSC 26001). The efficiency of each RNAi against GABA_BR_1 was assessed by RT-qPCR in flies expressing the RNAi with the pan-neuronal driver *elav*.

For calcium *in vivo* imaging, we used the *AOP-GCaMP3 (*gift from Barret Pfeiffer, Janelia Research Center) and *UAS-IVS-GCaMP3* [30] lines to construct the *AOP-GCaMP3,UAS-Shi* and *KK109166;UAS-IVS-GCaMP3* lines.

For immuno-histochemistry experiments, we used the *UAS-Syt-HA;;* [13] and *;;AOP-mCD8::GFP* (BDSC 32203) to construct the *UAS-Syt-HA;;AOP-mCD8::GFP* line.

CellPress

METHOD DETAILS

Behavior Experiments

For all behavior experiments, 0 – 2-day-old flies were transferred to fresh food vials one day before starvation. To induce RNAi expression, flies were kept at 30°C for 2 days before conditioning. Starvation lasted 21 h at 25°C, 16 h at 30°C (RNAi induction) or 24h at 20°C for the activation experiment to avoid activating TrpA1-expressing neurons during starvation period. Starved flied were only allowed access to mineral water and were then trained with one cycle of appetitive conditioning, consisting of exposure to one odour paired with a sugar reward (a 1.5 M sucrose (Sigma-Aldrich) solution in mineral water) and subsequent exposure to a second odour in the absence of sucrose, as previously described [23]. Odours were produced using 3-octanol (> 95% purity; Fluka 74878, Sigma-Aldrich) at 3.60×10^{-4} M, and 4-methylcyclohexanol (99% purity; Fluka 66360, Sigma-Aldrich) at 3.25×10^{-4} M diluted in paraffin oil (VWR), as previously described. The memory test was performed as described in [29] by exposing the flies to both odours simultaneously in a T-maze for 1 min. The performance index was calculated as the number of flies that avoided the conditioned odour minus the number of flies that avoided the unconditioned odour, divided by the total number of flies in the experiment. A single performance index value is the average of the scores from two groups of flies of the same genotype trained with either octanol or methylcyclohexanol as the conditioning stimulus.

For the experiment shown in Figure S2I, flies were transferred 45 minutes after appetitive conditioning in a barrel-type machine normally used for aversive conditioning and were delivered 12 pulses of 60V-electric shocks, each of 1.5 s duration, one pulse every 5 s.

Temperature-Shift Protocols

For sharp blockade of synaptic transmission after training, flies expressing Shi[ts] were conditioned on the second odor at the permissive temperature, and placed either immediately, 0.5 h, 0.75 or 1.5h after training in pre-warmed bottles at 33°C for 0.5 h, 0.75 h, 1 h or 1.5 h. Flies were then progressively returned to the permissive temperature (18°C for LTM and 25°C for STM experiments). Permissive-temperature control experiments were performed at 25°C. Time courses of the temperature shifts employed in each experiment have been provided alongside the graph of memory performance in each relevant figure.

To activate synaptic transmission during consolidation, flies expressing TrpA1 were trained at a permissive temperature (20°C), and placed either immediately or 0.5 h later in pre-warmed bottles at 30°C for 0.5 h and then return to 18°C until testing. Memory tests were performed 24 hr later at 20°C. For permissive-temperature control experiments starvation, conditioning and testing were performed at 20°C and flies were placed directly after conditioning at 18°C until testing. Time courses of the temperature shifts used in each experiment have been provided alongside the graph of memory performance in each relevant figure.

For RNAi expression in adult MBs, flies were maintained at 30.5°C for 2 days prior to training, after which experiments were performed at 25°C. For non-induced experiments, flies were placed at 18°C for 2 days prior to training and the experiments were then performed at 25°C. For LTM experiments, flies were stored at 18°C after acquisition, prior to testing.

Sugar Response Tests

Tests were performed on starved flies in a T-maze apparatus as previously described [23]]. Flies were trapped in either maze arm after 1min. The arm with sugar was placed alternately on the right or left. Sugar response was calculated as for the memory test and then used as a score. The sugar response tests were performed at 25°C (following 2 days of induction at 30.5°C for flies carrying the tub-GAL80[ts] transgene).

Olfactory Acuity

Tests were performed as previously described [29] at 25°C (following 2 days of induction at 30.5°C for flies carrying the tubGAL80[ts] transgene). Flies were starved for 21 hr (or 16 hr at 30.5°C for flies carrying the tubGAL80[ts] transgene) before the olfactory test. One odor was tested for 1 min against its solvent (paraffin oil). The response index was calculated as for the memory response test and then used as a score. The odor was delivered alternately through the right or left arm of the maze. A PI of 1 indicates complete behavioral repulsion.

Immuno-histochemistry experiments

30E11-LexA;R83A12-Gal4 females were cross with *UAS-Syt-HA;;AOP-mCD8::GFP* males to obtain *30E11-LexA;R83A12-Gal4 > UAS-Syt-HA;;AOP-mCD8::GFP* females. For the immune-histochemistery experiments, only the females were used because the genotype of the males from this cross is *30E11-LexA;R83A12-Gal4 > Y;;AOP-mCD8::GFP.* Prior to dissection, whole *30E11-LexA;R83A12-Gal4 > UAS-Syt-HA;;AOP-mCD8::GFP* females flies were fixed in 4% PFA (Electron Microscopy Science) in PBT (PBS containing 1% Triton X-100 (Sigma-Aldrich)) at 4°C overnight. Brains were dissected in *Drosophila* Ringer solution and fixed for 1 h at room temperature (RT) in 4% PFA in PBT. Samples were then rinsed three times for 20 min in PBT, blocked with 2% bovine serum albumin (EuroMedex) in PBT for 2 h and incubated with anti-GFP antibody at 1:400 (rabbit anti-GFP, Life Technologies), anti-HA antibody at 1:200 (rat anti-HA, Sigma/Roche) and anti-nc82 at 1:100 (mouse anti-nc82, DSHB) in the blocking solution at 4°C overnight. After rinsing, brains were incubated with secondary antibodies at 1:400 (anti-rabbit conjugated to AlexA Fluor 488, anti-rat conjugated to AlexA Fluor 595 and anti-mouse conjugated to AlexA Fluor 647, Life Technologies) in the blocking solution for 3h at RT. After rinsing, brains were mounted in Prolong Mounting Medium (Life Technologies) for microscopy analysis. Images were acquired with a Nikon A1R confocal microscope. Confocal Z stacks were acquired in 1 μm slices and imported into NIH Fiji for analyses.

In Vivo Calcium Imaging

Female flies were caught without anesthesia, then glued and operated for *in vivo* confocal imaging [30] and subsequent data analysis of spontaneous activity as described in a previously detailed protocol [12]. The proboscis was also glued to the thorax to limit motion artifacts during image acquisition. The recording chamber was then placed beneath the water immersion 20 × objective (Olympus), the brain of the fly being thus observed from the top. Experiments were performed at 20°C, and the aperture on the top of the fly head was bathed in a continuously flowing perfusion of *Drosophila* Ringer's solution (130 mM NaCl, 5 mM KCl, 2 mM $MgCl_2$, 2 mM $CaCl_2$, 36 mM ribose, 5 mM HEPES-NaOH; pH 7.3; 305 mOsm, all chemicals from Sigma-Aldrich). Shi^{ts} experiments: *30e11-LexA;R83A12-Gal4* or *30e11-LexA;+* females were crossed to *Aop-GCaMP3;UAS-shi^{ts}* males. The progeny was kept at 25°C throughout. $GABA_BR_1$ RNAi experiments: *Tubulin-GAL80^{ts};NP0047-Gal4* or *Tubulin-GAL80^{ts};+* females were crossed to *UAS-GABA_BR_1^{RNAi1};UAS-IVS-GCaMP3* males. The progeny was kept at 18°C throughout development and adult flies were put at 30.5°C 2d before the experiment to strongly induce RNAi expression.

Starvation protocols were the same as for behavior experiments (20 h at 25°C for Shi^{ts} experiments or 16h at 30.5°C for $GABA_BR_1$ experiments), and flies were trained with one cycle of appetitive conditioning or an unpaired protocol at 25°C. Except in Figure S4I-M where Methylcyclohexanol was used, imaging experiments were performed using the Octanol as the odorant for paired association with sugar; consequently, Octanol was the first odorant presented after the presentation of sucrose in the unpaired protocol. For Shi^{ts} experiments, flies were either immediately imaged or kept at 25°C or 33°C for 1 h or at 25°C for 0.5 h then at 33°C for 0.5h before dissection and imaging. Time courses of the temperature shifts employed in each experiment have been provided alongside the illustrative examples of MP1 neuron recording. For $GABA_BR_1$ RNAi experiments flies were kept at 25°C for 1 hr before dissection and imaging.

For each fly, 1000-image recording were done with a rate of one image every 125 ms. MP1 neuron activity was reported from the normalized fluorescence variations (ΔF/F0) in MB projections. As previously described in [12]], image analysis was performed offline with a custom-written MATLAB program. Light intensity was averaged over a region of interest delimited by hand and surrounding the projections of MP1 dopaminergic neurons on the mushroom bodies in the observed plane. From a given region of interest, the resulting time trace was normalized to a percent change of fluorescence (100 *(F − F0) / F0), using a baseline value of the fluorescence F0 that was estimated as the mean fluorescence over the whole acquisition. To remove long-term drift, a baseline resulting from the moving average over a 100 s time window was then subtracted from the signal. Thus, in subsequent frequency analyses, all frequency axes are presented starting at 0.01 Hz. Given that signals are noisy, their amplitudes were estimated as the difference between the means of the 30% upper and lower quantiles of data points. For each signal, the power spectrum was computed and smoothed over a frequency window of 0.02 Hz. Rhythmic spontaneous activity in the time domain resulted in a peak in the power spectrum that had a finite width, as oscillations are intrinsically noisy. A fit of a Lorentzian curve to the power spectrum was performed to yield an estimate of the central frequency of the peak, f0, and the width of the peak at half its maximal value, Δf. f0 defined the characteristic frequency of the oscillation and frequency fluctuations around f0, and hence the regularity of the oscillation, could be quantified by the quality factor Q = f0/Δf. A quality factor greater than 0.5 indicates that the zero frequency is excluded from the peak: this value was thus taken as a threshold to define a signal as rhythmically oscillating. When the fitting procedure converged to a value below 0.5, it was thus irrelevant to define oscillating parameters, and f0 and Q were both assigned zero values.

Quantitative PCR analyses

Quantitative PCR analyses to assess the efficiency of the two $GABA_BR_1$ RNAi lines were performed as described in [56]. For *elav* genotypes, flies were raised at 25°C. Total RNA was extracted from 60 female heads using the RNeasy Plant Mini Kit (QIAGEN). Preparation were submitted to a DNaseI treatment (New England Biolabs) for 15 min at 37°C. DNase was heat inactivated with EDTA (10 mM). Samples were cleaned with the RNA Minielute Cleanup kit (QIAGEN) and reverse-transcribed with oligo(dT)20 primers using the SuperScript III First-Strand kit (Thermofisher/Invitrogen) according to the manufacturer's instructions. Level of the target cDNA $GABA_BR_1$ was compared against level of α-Tub84B (Tub, CG1913) cDNA, which was used as a reference. Amplification was performed using a LightCycler 480 (Roche) and the SYBR Green I Master mix (Roche). Reactions were carried out in triplicate. Specificity and size of amplification products were assessed by melting curve analyses and agarose gel electrophoresis, respectively. Expression relative to reference is expressed as a ratio ($2^{-\Delta Cp}$, where Cp is the crossing point).

QUANTIFICATION AND STATISTICAL ANALYSIS

All data are presented as means ± SEM. Comparisons between 2 groups were performed using a two-tailed unpaired t test; results are provided as the value t of the t distribution with x degrees of freedom obtained from the data. Comparisons between multiple groups were performed using one-way ANOVA followed by Newman-Keuls pairwise comparisons. ANOVA results are given as the value of the Fisher distribution F(x,y) obtained from the data, where x is the numerator degrees of freedom and y is the denominator degrees of freedom. Asterisks denote the smallest significant difference between the relevant group and its controls with the post hoc comparisons (*$p < 0.05$, **$p < 0.01$, *ns*: not significant). When comparisons between multiple groups was not possible using the one-way ANOVA, which was the situation only for the analysis of the qPCR experiments (figure S4D), a Mann Whitney test was performed to compare each experimental group to the control group and Bonferroni correction was applied to adjusted the significance.